Journal of Solid State Chemistry 184 (2011) 337–342

Contents lists available at ScienceDirect

Journal of Solid State Chemistry

journal homepage: www.elsevier.com/locate/jssc

Syntheses and single-crystal structures of $CsTh(MoO_4)_2Cl$ and $Na_4Th(WO_4)_4$

Geng Bang Jin, L. Soderholm *

Chemical Sciences and Engineering Division, CHM/200 Argonne National Laboratory, 9700 S. Cass Ave., Argonne, IL 60439, United States

ARTICLE INFO

Article history:
Received 30 September 2010
Received in revised form
17 November 2010
Accepted 1 December 2010
Available online 5 December 2010

Keywords:
Thorium
Molybdate
Tungstate
Insertion compound
Single-crystal structure

ABSTRACT

Colorless crystals of $CsTh(MoO_4)_2Cl$ and $Na_4Th(WO_4)_4$ have been synthesized at 993 K by the solid-state reactions of ThO_2, MoO_3, CsCl, and $ThCl_4$ with Na_2WO_4. Both compounds have been characterized by the single-crystal X-ray diffraction. The structure of $CsTh(MoO_4)_2Cl$ is orthorhombic, consisting of two adjacent $[Th(MoO_4)_2]$ layers separated by an ionic CsCl sublattice. It can be considered as an insertion compound of $Th(MoO_4)_2$ and reformulated as $Th(MoO_4)_2 \cdot CsCl$. The Th atom coordinates to seven monodentate MoO_4 tetrahedra and one Cl atom in a highly distorted square antiprism. $Na_4Th(WO_4)_4$ adopts a scheelite superlattice structure. The three-dimensional framework of $Na_4Th(WO_4)_4$ is constructed from corner-sharing ThO_8 square antiprisms and WO_4 tetrahedra. The space within the channels is filled by six-coordinate Na ions. Crystal data: $CsTh(MoO_4)_2Cl$, monoclinic, $P2_1/c$, $Z=4$, $a=10.170(1)$ Å, $b=10.030(1)$ Å, $c=9.649(1)$ Å, $\beta=95.671(2)^\circ$, $V=979.5(2)$ Å^3, $R(F)=2.65\%$ for $I>2\sigma(I)$; $Na_4Th(WO_4)_4$, tetragonal, $I4_1/a$, $Z=4$, $a=11.437(1)$ Å, $c=11.833(2)$ Å, $V=1547.7(4)$ Å^3, $R(F)=3.02\%$ for $I>2\sigma(I)$.

1. Introduction

Actinide molybdate and tungstate compounds have been extensively studied for a few decades [1–20]. Molybdenum is one of the significant fission products that forms during an irradiation of nuclear fuel in a reactor and as such reactions between molybdenum, actinides and other fission products can affect the behavior of the fuel. Actinide molybdates may also be important for the long-term evolution of nuclear waste in a geological repository. From a more fundamental perspective, actinide molybdates and tungstates have shown extremely rich structural chemistries, especially the uranium (VI) phases owing to the diverse coordination geometries of uranyl, molybdenum (VI) and tungsten (VI) ions [13–15]. For example, the approximately linear uranyl cation (UO_2^{2+}) can coordinate with four to six equatorial oxides, while the coordination environment for the Mo^{6+} cation varies from fourfold to sixfold. Metal-oxide polyhedra connect via common vertices to form a range of structures, including isolated clusters, chains, sheets and frameworks. Compared to uranyl compounds, fewer structural studies have been conducted on molybdates and tungstates containing the lower-valent actinides Th(IV), U(IV), Np(IV), Pu(IV) and Am(III) [17–20]. Their coordination numbers vary considerably; Th(IV), for example, has ten coordinating water molecules in the homoleptic $[Th(H_2O)_{10}]^{4+}$ ion [21], but the coordination number can vary between six and twelve for oxidic systems [22]. With respect to molybdates or tungstates, lower-valent actinides usually coordinate to eight or nine oxide atoms, and further connect through the polyhedra of molybdates or tungstates to form three-dimensional structures. Most studies on lower-valent actinide molybdates or tungstates were conducted more than two decades ago.

Recently, nuclear fuel cycles using the more abundant thorium have been reconsidered, which is spurring more interest in reexamining and exploring the Th oxometalate system [23–25]. Most thorium molybdate or tungstate studies have focused on quaternary phases containing alkali metals. These systems have been studied by means of liquid–solid phase diagrams, X-ray diffraction and thermal analysis. Numerous compounds have been identified, including $Li_2Th_4(MO_4)_9$ (M=Mo, W) [1,4], $A_2Th(MO_4)_3$ (A=Na, K, Rb, Cs; M=Mo, W) [1,4–10,18], $A_4Th(MO_4)_4$ (A=Na, K, Rb, Cs; M=Mo, W) [1,4–7,9,10,18], $A_8Th(MoO_4)_6$ (A=K, Rb) [4–6]. $Li_2Th_4(MO_4)_9$ is isostructural with $Cu_2Th_4(MoO_4)_9$, which consists of corner-sharing ThO_9 polyhedra and MoO_4 tetrahedra [26]. The series of $A_2Th(MO_4)_3$ adopts a scheelite ($CaWO_4$)-type structure [18,27] with A and Th atoms occupying the eight-coordinate Ca positions in a ordered manner [18,28]. M atoms are surrounded by four oxygen atoms in a distorted tetrahedron. Similarly, $A_4Th(MO_4)_4$ (A=Na, K) crystallizes in a scheelite superlattice structure with an ordering between A and Th over the Ca sites and four M atoms distributed in five W positions [18,29]. $A_4Th(MO_4)_4$ (A=Rb, Cs) has only been characterized by powder X-ray diffraction and the structural details are not known [6,7,10]. The structure of $A_8Th(MoO_4)_6$ is related to that of palmierite ($K_2Pb(SO_4)_2$) [30] with A and Th atoms ordered over the Pb sites [31]. Here, we present the synthesis and structure of a new cesium thorium molybdate compound, $CsTh(MoO_4)_2Cl$. We also report a different synthetic route for $Na_4Th(WO_4)_4$ and its single-crystal

* Corresponding author.
E-mail address: LS@anl.gov (L. Soderholm).

0022-4596/$ - see front matter © 2010 Elsevier Inc. All rights reserved.
doi:10.1016/j.jssc.2010.12.003

structure. Because of our interest in the heavier actinides, we have purposefully designed a synthetic route that can be used with redox-active cations.

2. Experiments

2.1. Syntheses

ThO_2 (International Bio-Analytical Industries, Inc.), $ThCl_4$ (International Bio-Analytical Industries, Inc.), MoO_3 (Cerac, 99.5%), CsCl (Strem Chemicals, 99.999%) and Na_2WO_4 (MP Biomedicals) were used as received.

Caution!: ^{232}Th is an α emitting radioisotope and as such is considered a health risk. Its use requires appropriate infrastructure and personnel trained in the handling of radioactive materials. For both reactions, the reactants were loaded into fused-silica ampoules and then flame-sealed under vacuum. The reaction mixtures were placed in a computer-controlled furnace and heated to 993 K in 48 h, held at this temperature for 120 h, slowly cooled to 693 K in 150 h, and then cooled to 298 K in 6 h. The reaction products were washed with water and dried with acetone. Crystals found in these reactions were characterized by single-crystal X-ray diffraction.

$CsTh(MoO_4)_2Cl$: 0.015 g (0.057 mmol) of ThO_2 and 0.020 g (0.14 mmol) of MoO_3 were thoroughly ground together before loading into a fused-silica ampoule with 0.080 g (0.48 mmol) of CsCl. The reaction products included a large number of colorless crystals of $CsTh(MoO_4)_2Cl$ and violet-colored prisms of MoO_2 [32]. Both compounds are stable in air. The yield of $CsTh(MoO_4)_2Cl$ is difficult to estimate, due to similar appearance of crystals and broken glass pieces. This will be less of a problem when this synthetic route is applied to the heavier actinides, which are expected to form easily distinguishable colored phases.

$Na_4Th(WO_4)_4$: this compound was obtained from the reaction of 0.020 g (0.053 mmol) of $ThCl_4$ and 0.090 g (0.31 mmol) of Na_2WO_4. Colorless polyhedral crystals of $Na_4Th(WO_4)_4$ were the only product identified. The yield of $Na_4Th(WO_4)_4$ is difficult to estimate, due to similar appearance of colorless crystals and broken glass pieces.

2.2. Structure determination

Single-crystal X-ray diffraction data for $CsTh(MoO_4)_2Cl$ and $Na_4Th(WO_4)_4$ were collected with the use of graphite-monochromatized MoKα radiation (λ=0.71073 Å) at 100 K on a Bruker APEX2 diffractometer [33]. The crystal-to-detector distance was 5.106 cm. Data were collected by a scan of 0.3° in ω in groups of 600 frames at φ settings of 0°, 90°, 180° and 270°. The exposure time was 20 s/frame. The collection of intensity data as well as cell refinement and data reduction were carried out with the use of the program APEX2 [33]. Absorption corrections, incident beam, and decay corrections were performed with the use of the program SADABS [34]. The structures were solved with the direct-methods program SHELXS and refined with the least-squares program SHELXL [35]. The program STRUCTURE TIDY [36] was used to standardize the positional parameters. Additional experimental details are given in Table 1 and in the Supporting material.

Table 1
Crystal data and structure refinements for $CsTh(MoO_4)_2Cl$ and $Na_4Th(WO_4)_4$[a,b].

	$CsTh(MoO_4)_2Cl$	$Na_4Th(WO_4)_4$
Fw	720.28	1315.40
Crystal system	monoclinic	tetragonal
Space group	$P2_1/c$	$I4_1/a$
a (Å)	10.170(1)	11.437(1)
b (Å)	10.030(1)	/
c (Å)	9.649(1)	11.833(2)
β (°)	95.671(2)	/
V (Å^3)	979.5(2)	1547.7(4)
ρ_c (g/cm^3)	4.884	5.645
μ (cm^{-1})	216.10	393.84
$R(F)^c$	0.0265	0.0302
$R_w(F_o^2)^d$	0.0597	0.0706

[a] For both structures, Z=4, λ=0.71073 Å and T=100(2) K.
[b] For $Na_4Th(WO_4)_4$, from X-ray diffraction powder data in Ref. [1]: a=11.47 Å and c=11.86 Å; in Ref. [4]: a=11.44 Å and c=11.80 Å.
[c] $R(F)=\Sigma||F_o|-|F_c||/\Sigma|F_o|$ for $F_o^2 > 2\sigma(F_o^2)$.
[d] $R_w(F_o^2)=\{\Sigma[w(F_o^2-F_c^2)^2]/\Sigma wF_o^4\}^{1/2}$ for all data. $w^{-1}=\sigma^2(F_o^2)+(qF_o^2)^2$ for $F_o^2 \geq 0$; $w^{-1}=\sigma^2(F_o^2)$ for $F_o^2 < 0$. q=0.0296 for $CsTh(MoO_4)_2Cl$, 0.0331 for $Na_4Th(WO_4)_4$.

3. Results

3.1. Syntheses

Assuming that the principle route to alkali metal thorium molybdates or tungstates in a nuclear reactor is the reaction of the fuel with fission products, these phases have been prepared via solid-state reactions of the oxides [1,4–7,9,10]. Some of the reactions required high temperatures and only resulted in powder samples, due to the high melting points of the oxides. Halides such as fluoride are another potential form of thorium fuel [24]. Therefore, we are also interested in their use as starting materials. Halides generally have lower melting points than oxides. For example, the melting points of ThO_2 and $ThCl_4$ are 3663 and 1038 K, respectively. In the synthesis of $CsTh(MoO_4)_2Cl$, the reactant CsCl, with a melting point of 918 K, was used as the Cs source and Cl is incorporated into the final product. Excess of CsCl served as the flux and excess MoO_3 were added due to the formation of the byproduct MoO_2. Carbon coating inside of the silica ampoule is a possible reducing agent for MoO_3, as most of the coating was gone after the reaction.

The syntheses of $Na_4Th(WO_4)_4$ have been reported from reactions between Na_2CO_3, WO_3, and ThO_2 [1] or between Na_2WO_4 and $Th(WO_4)_2$ [4]. We used $ThCl_4$ as the Th source for the preparation of $Na_4Th(WO_4)_4$, which can be described by the following reaction:

$$ThCl_4 + 4Na_2WO_4 \rightarrow Na_4Th(WO_4)_4 + 4NaCl$$

Similar solid-state metathesis reactions have been used to prepare actinide pnictides and chalcogenides [37]. The driving force of this reaction is the formation of a highly stable NaCl lattice. Excess of Na_2WO_4 (melting point: 971 K) served as the flux.

3.2. Structures

$CsTh(MoO_4)_2Cl$ crystallizes in the space group $P2_1/c$ with a two-dimensional layered structure, as shown in Fig. 1. The structure of $CsTh(MoO_4)_2Cl$ consists of alternating layers of $[Th(MoO_4)_2]$ and [CsCl] in the *bc* plane. Fig. 2a shows the coordination environment surrounding the Th atom. Each Th atom connects to four $Mo(1)O_4$ tetrahedra, three $Mo(2)O_4$ tetrahedra, and one Cl atom. The polyhedron of ThO_7Cl forms a highly distorted square antiprism, due to the much longer Th–Cl distance relative to the Th–O distances. Each $Mo(1)O_4$ tetrahedron share corners with four ThO_7Cl square antiprisms, while each $Mo(2)O_4$ tetrahedron shares corners with three ThO_7Cl square antiprisms to form a $[Th(MoO_4)_2]$ layer, as shown in Fig. 2b. Each O atom is shared by one ThO_7Cl square antiprism and one MoO_4 tetrahedron, except the terminal O(8) atom from the $Mo(2)O_4$ tetrahedron. Cs^+ cations are surrounded by five O^{2-} and four Cl^- anions.

Selected bond distances for $CsTh(MoO_4)_2Cl$ are listed in Table 2. Th–O distances range from 2.379(3) to 2.424(3) Å, which are close to

those of 2.360(4) to 2.459(4) Å in $Th(MoO_4)_2$ [38]. The Th–Cl distance, 2.808(1) Å, is comparable to those of 2.718(8) and 2.903(7) Å found for eight-coordinate Th^{4+} cations in $ThCl_4$ [39]. Mo–O distances are in the range 1.711(3)–1.792(3) Å and O–Mo–O angles are between 106.0(2) and 116.3(2)°. Mo(2)–O(8) has the shortest distance of 1.711(3) Å compared to the rest ones, which is expected for a terminal O. Overall they are close to those of 1.743(4)–1.778(4) Å and 106.4(2)–111.8(2)° found in $Th(MoO_4)_2$ [38]. Cs–O distances are in the range 3.061(3)–3.586(3) Å, and Cs–Cl distances are in the range 3.467(1)–3.652(1) Å. The structure of $CsTh(MoO_4)_2Cl$ includes discrete ThO_7Cl square antiprisms and MoO_4 tetrahedra, which results in relative long Th–Th (5.4224(6) Å) and Mo–Mo (3.8853(6) Å) distances. For example, the Th–Th distance between two edge-sharing ThO_8 cubes in ThO_2 [40] is only 3.958 Å. The Th–Mo distance between the corner-sharing ThO_7Cl and MoO_4 polyhedra is 3.7846(6) Å.

The structure of $CsTh(MoO_4)_2Cl$ is closely related to that of orthorhombic $Th(MoO_4)_2$, which is constructed from similar layers of $[Th(MoO_4)_2]$ (Fig. 3) [38]. A Th atom in $Th(MoO_4)_2$ is surrounded by seven MoO_4 tetrahedra within a single layer of $[Th(MoO_4)_2]$, and it further connects to one MoO_4 tetrahedron from the adjacent layer to complete its coordination environment as a slightly distorted square antiprism. $[Th(MoO_4)_2]$ layers are stitched together by this additional Th–O bonding to form the three-dimensional structure of $Th(MoO_4)_2$. The structure of $CsTh(MoO_4)_2Cl$ can be obtained by inserting an ionic [CsCl] layer and breaking this additional Th–O bonding between those $[Th(MoO_4)_2]$ layers in $Th(MoO_4)_2$. The Th–Th interplanar distance increases from 6.394(2) to 7.4084(9) Å with the insertion of the CsCl layer. Similar salt-inclusion reactions have been reported using the molten-salt methods, which have resulted in a class of hybrid materials of mixed covalent and ionic lattices [41,42]. In this case, the ionic [CsCl] layer can be considered to support the more covalent layer of $[Th(MoO_4)_2]$. The chemical formula of $CsTh(MoO_4)_2Cl$ can also be expressed as $Th(MoO_4)_2 \cdot CsCl$.

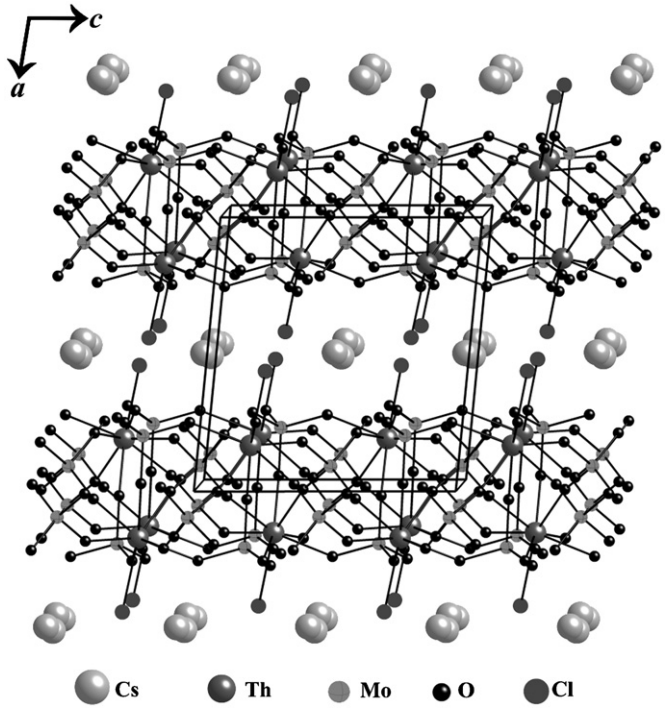

Fig. 1. A view of the two-dimensional layered structure of $CsTh(MoO_4)_2Cl$ down the *b* axis.

Table 2
Selected interatomic distances (Å) for $CsTh(MoO_4)_2Cl$.

Cs(1)–O(4)	3.586(3)	Th(1)–O(6)	2.379(3)
Cs(1)–O(5)	3.061(3)	Th(1)–O(7)	2.399(3)
Cs(1)–O(6)	3.402(4)	Th(1)–Cl(1)	2.808(1)
Cs(1)–O(7)	3.211(3)	Mo(1)–O(1)	1.761(3)
Cs(1)–O(8)	3.229(4)	Mo(1)–O(2)	1.768(3)
Cs(1)–Cl(1)	3.467(1)	Mo(1)–O(4)	1.759(3)
Cs(1)–Cl(1)	3.523(1)	Mo(1)–O(5)	1.779(3)
Cs(1)–Cl(1)	3.594(1)	Mo(2)–O(3)	1.772(3)
Cs(1)–Cl(1)	3.652(1)	Mo(2)–O(6)	1.792(3)
Th(1)–O(1)	2.424(3)	Mo(2)–O(7)	1.788(3)
Th(1)–O(2)	2.383(3)	Mo(2)–O(8)	1.711(3)
Th(1)–O(3)	2.392(3)	Th(1)–Th(1)	5.4224(6)
Th(1)–O(4)	2.398(3)	Th(1)–Mo(1)	3.7846(6)
Th(1)–O(5)	2.415(3)	Mo(1)–Mo(2)	3.8853(6)

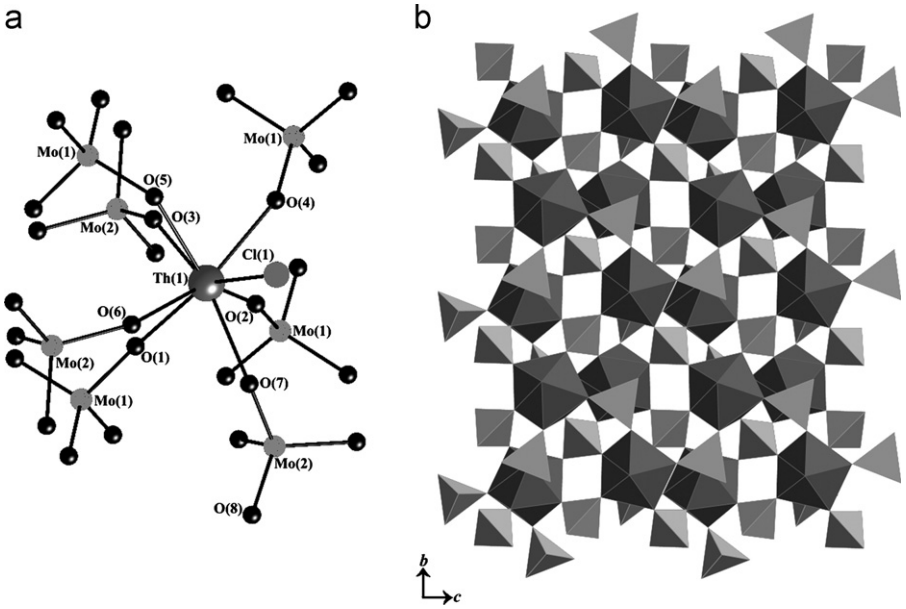

Fig. 2. (a) An illustration of the coordination environment for the Th atom in $CsTh(MoO_4)_2Cl$ and (b) a polyhedral presentation of an individual $[Th(MoO_4)_2]$ layer in the *bc* plane.

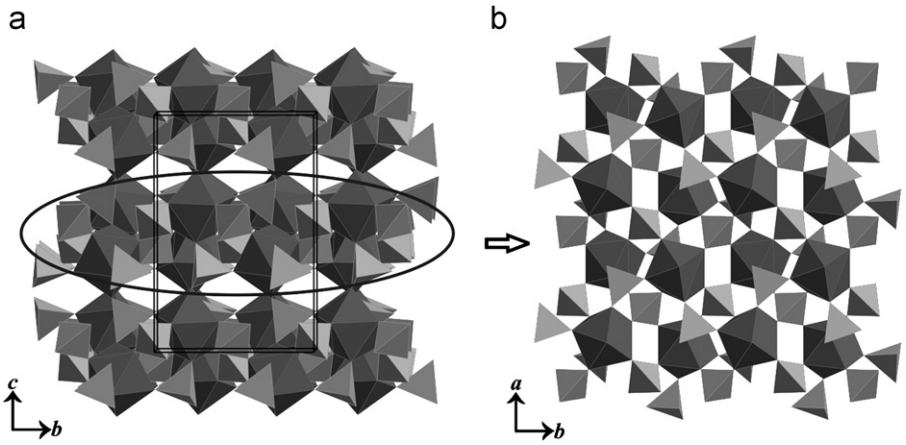

Fig. 3. (a) Structure of orthorhombic $Th(MoO_4)_2$ constructed by $[Th(MoO_4)_2]$ layers (circled) with additional Th–O bonding between the layers and (b) A depiction of an individual $[Th(MoO_4)_2]$ layer consists of ThO_8 square antiprisms and MoO_4 tetrahedra.

Table 3
Selected interatomic distances (Å) for $Na_4Th(WO_4)_4$.

Na(1)–O(1)	2.463(6)	W(1)–O(1)	1.813(5)
Na(1)–O(2)	2.461(6)	W(1)–O(2)	1.830(5)
Na(1)–O(3)	2.355(6)	W(1)–O(3)	1.746(5)
Na(1)–O(3)	2.467(6)	W(1)–O(4)	1.753(5)
Na(1)–O(4)	2.370(6)	Th(1)–Th(1)	6.4381(6)
Na(1)–O(4)	2.448(6)	Th(1)–W(1)	3.7946(5)
Th(1)–O(1) × 4	2.411(5)	W(1)–W(1)	4.0654(7)
Th(1)–O(2) × 4	2.402(5)		

$Na_4Th(WO_4)_4$ has been previously characterized by the powder X-ray diffraction [1,4]; however, only the unit cell has been indexed and no structural information has been reported. Given similar cell parameters, $Na_4Th(WO_4)_4$ has been considered to be isotypic with other $A_4An(MO_4)_4$ (A=Li, Na, K; An=Th, U, Np, Pu; M=Mo, W) compounds, which adopt a scheelite superlattice structure [18,19,29,43]. Our single-crystal structural results for $Na_4Th(WO_4)_4$ generally agree with those deduced from the powder studies, but are much more precise (Tables 1 and 3). As shown in Fig. 4, The cell vectors of $Na_4Th(WO_4)_4$ are related to that of $CaWO_4$ [27]: $a=2a_s+b_s$, $b=-a_s+2b_s$, $c=c_s$, where s represents scheelite. To be consistent with $CaWO_4$, $Na_4Th(WO_4)_4$ can be reformulated to recognize it as the defect scheelite $(Na_{4/5}Th_{1/5})[\square_{1/5}(WO_4)_{4/5}]$. In the structure of $Na_4Th(WO_4)_4$, 4/5 of the eight-coordinate Ca sites in $CaWO_4$ are occupied by Na atoms and the rest of 1/5 of Ca sites are occupied by Th atoms. Meanwhile, 1/5 of W sites in $CaWO_4$ are vacant in the $Na_4Th(WO_4)_4$ structure. Each Th atom is connected to eight WO_4 tetrahedra in a square antiprism (Fig. 5), while each WO_4 tetrahedron share corners with two ThO_8 square antiprisms to form the three-dimensional framework of $Na_4Th(WO_4)_4$. The space within the channels is filled by Na^+ counter cations. Each Na^+ cation is only surrounded by six close O neighbors, due to the vacancy of the WO_4 tetrahedra.

Selected bond distances for $Na_4Th(WO_4)_4$ are listed in Table 3. Th–O distances are 2.411(5) and 2.402(5) Å, which are close to those of 2.42(2) and 2.39(2) Å in $Na_4Th(MoO_4)_4$ [18]. W–O distances are in the range of 1.746(5) and 1.830(5) Å and O–W–O angles are between 106.6(2) and 112.7(2)°. They are comparable to those of 1.78(1) Å and 107.5 to 113.4° found in $CaWO_4$ [27]. Na–O distances are in the range 2.355(6)–2.463(6) Å for NaO_6 polyhedron, and there is a much longer contact with a Na–O distance of 3.585(6) Å, which is probably too long to be considered as any interaction. The Th–Th distance between two discrete ThO_8 square antiprisms is 6.4381(6) Å and the W–W distance between two discrete WO_4 tetrahedra is 4.0654(7) Å. The Th–W distance between the corner-sharing ThO_8 and WO_4 polyhedra is 3.7946(5) Å.

4. Discussion

The structure of $CsTh(MoO_4)_2Cl$ consists of layers of $[Th(MoO_4)_2Cl]^-$ separated by Cs^+ cations. Significant intercalative ion-exchange reactions have been observed in a number of other layered actinide compounds [44,45] that have shown promising applications for the remediation of nuclear waste [46]. The stable $[Th(MoO_4)_2Cl]^-$ structure is another example of a layered material that may serve as a good ion-exchange host for the $^{135}Cs^+$ cation, a long-lived nuclear fission product. Based on the reasonable Cs–O and Cs–Cl distances, and representative Cs^+ thermal parameters, the size of the Cs^+ cation fits into the space between the $[Th(MoO_4)_2Cl]^-$ layers, which should give a preference to the Cs^+ cations over other smaller alkali metal cations during an ion-exchange reaction. It would be worthwhile to prepare the corresponding heavier actinide phases and study how their electronic and magnetic structures respond to the insertion of a salt layer.

As stated earlier, both structures $A_2Th(MO_4)_3$ (A=Na, K, Rb, Cs; M=Mo, W) and $A_4Th(MO_4)_4$(A=Na, K; M=Mo, W) are related to scheelite, $CaWO_4$. The formula of $A_2Th(MO_4)_3$ can be rewritten as $(A_{2/3}Th_{1/3})(MO_4)$ with A and Th atoms occupying the eight-coordinate Ca positions, while $A_4Th(MO_4)_4$ can be reformulated as $(A_{4/5}Th_{1/5})[\square_{1/5}(MO_4)_{4/5}]$ with an ordering between A and Th over the Ca sites and 1/5 vacancy of the MO_4 units. Scheelite materials especially those containing Bi have been well known for their catalytic activity in the chemical oxidation reactions [47]. They have been also studied as electrode materials for solid-state fuel cells [48]. Both applications involve the oxygen transport in a bulk material, which is highly depending on the oxygen vacancies and the cations around them. The transport properties of those materials can be tuned by doping different valent metal cations. These potential catalytic and oxygen transport characteristics could have important implications for nuclear fuel applications, in which the complex chemistry will produce a variety of doped and defected structures with an unknown consequence.

5. Conclusions

A new cesium thorium molybdate, $CsTh(MoO_4)_2Cl$, was synthesized and single crystals of $Na_4Th(WO_4)_4$ were grown by using chlorides as starting materials. In the reaction for $CsTh(MoO_4)_2Cl$, the reactant CsCl was incorporated into the final product, which resulted in a hybrid material of mixed covalent and ionic lattices. In the structure of $CsTh(MoO_4)_2Cl$, the more covalent $[Th(MoO_4)_2]$ layers are separated by ionic [CsCl] layers. A similar $[Th(MoO_4)_2]$ layer has been observed in $Th(MoO_4)_2$, in which structure the $[Th(MoO_4)_2]$ layers are further

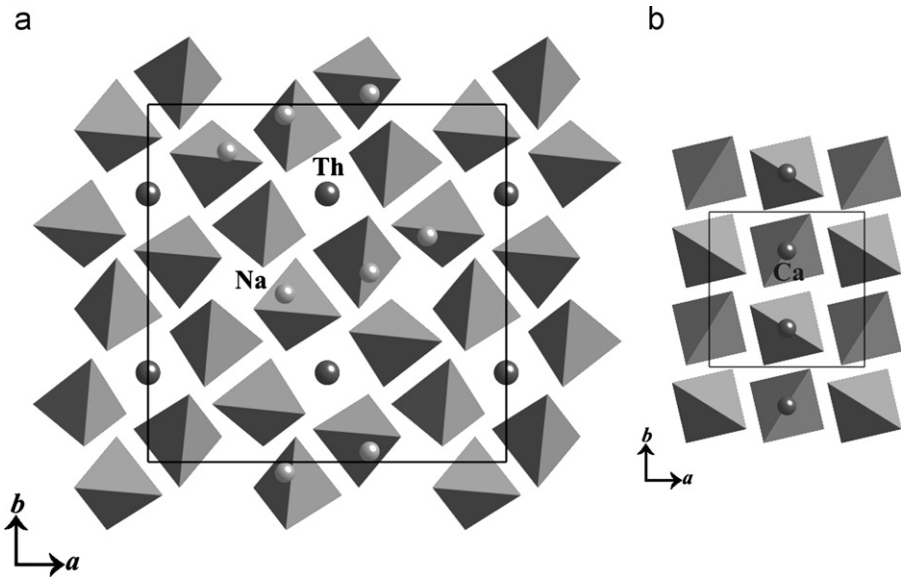

Fig. 4. A comparison between a unit cell of $Na_4Th(WO_4)_4$ (a) and that of $CaWO_4$ (b). WO_4 is shown in tetrahedron. The Th–O bonding, interactions between Na and O in $Na_4Th(WO_4)_4$, and interactions between Ca and O in $CaWO_4$ are omitted for the purpose of clarity.

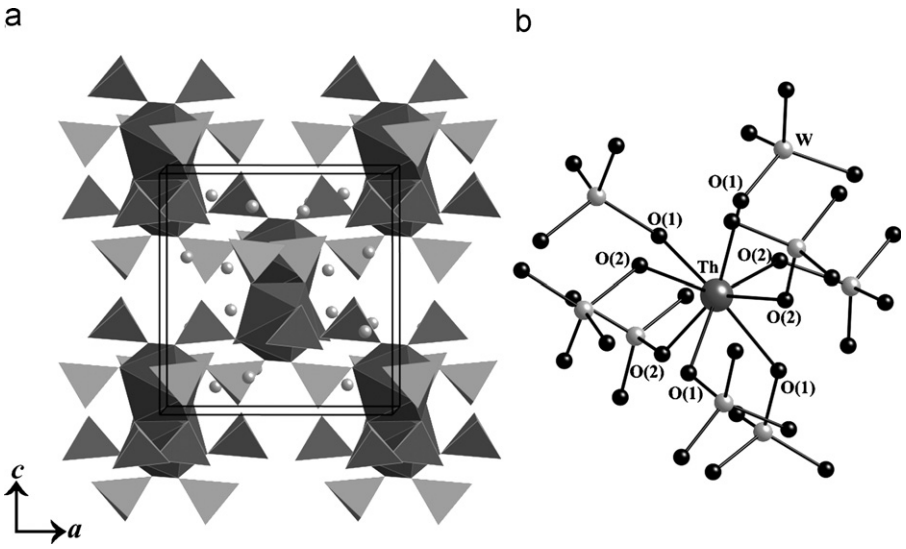

Fig. 5. (a) A unit cell of $Na_4Th(WO_4)_4$ along the *b* axis and (b) an illustration of the coordination environment for the Th atom.

connected by an additional Th–O bonding. The current structure studies of $CsTh(MoO_4)_2Cl$ and $Na_4Th(WO_4)_4$ confirm the dominance of eight-coordinate Th in a square antiprismatic geometry in thorium molybdate or tungstate compounds. However, the mono Th–O–Mo/W bond is very flexible with a range of bond angles that has resulted in different networks. As demonstrated in uranyl molybdates, the size of the alkali metal and other metal cations can largely influences the topology and geometry of the uranyl molybdate units. These results imply that rich structural variations of thorium molybdates or tungstates await discovery.

Supporting material

The crystallographic files in CIF format for $CsTh(MoO_4)_2Cl$ and $Na_4Th(WO_4)_4$ have been deposited with FIZ Karlsruhe as CSD nos. 422184 and 422185, respectively. These may be obtained free of charge by contacting FIZ Karlsruhe at +497247808 666 (fax) or crysdata@fiz-karlsruhe.de (e-mail).

Acknowledgments

This work is supported by the U.S. DOE, OBES, Chemical Sciences, Geosciences, and Biosciences Division under Contract DE-AC02-06CH11357.

Appendix A. Supporting information

Supplementary data associated with this article can be found in the online version at doi:10.1016/j.jssc.2010.12.003.

References

[1] V.K. Trunov, N.N. Bushuev, Radiokhimiya 11 (1968) 245.
[2] A. Tabuteau, M. Pages, W. Freundlich, Mater. Res. Bull. 7 (1972) 691.
[3] M.R. Lee, P. Mahe, C. R. Acad. Sci. Paris, C 279 (1974) 1137.
[4] J. Thoret, Rev. Chim. Mine´r. 11 (1974) 237.
[5] N.N. Bushuev, V.K. Trunov, A.R. Gizhinskii, Zh. Neorg. Khim. 20 (1975) 604.
[6] N.N. Bushuev, V.K. Trunov, Zh. Neorg. Khim. 20 (1975) 1143.

[7] N.N. Bushuev, V.K. Trunov, Zh. Neorg. Khim. 20 (1975) 1233.
[8] N.N. Bushuev, V.K. Trunov, Kristallografiya 21 (1976) 69.
[9] N.N. Bushuev, Zh. Neorg. Khim. 22 (1977) 1912.
[10] N.N. Bushuev, Zh. Neorg. Khim. 22 (1977) 2215.
[11] A. Tabuteau, M. Pages, J. Inorg. Nucl. Chem. 42 (1980) 401.
[12] T.L. Cremers, P.G. Eller, R.A. Penneman, C.C. Herrick, Acta Crystallogr. Sect. C 39 (1983) 1163.
[13] S.V. Krivovichev, Eur. J. Inorg. Chem. (2010) 2594.
[14] S. Obbade, C. Dion, E. Bekaert, S. Yagoubi, M. Saadi, F. Abraham, J. Solid State Chem. 172 (2003) 305.
[15] E.V. Alekseev, S.V. Krivovichev, W. Depmeier, O.I. Siidra, K. Knorr, E.V. Suleimanov, E.V. Chuprunov, Angew. Chem.-Int. Ed. 45 (2006) 7233.
[16] M. Grigor'ev, A. Fedoseev, N. Budantseva, M. Antipin, Radiokhimiya 47 (2005) 500.
[17] S. Dash, Z. Singh, N.D. Dahale, R. Prasad, V. Venugopal, J. Alloys Compd. 347 (2002) 301.
[18] N.D. Dahale, M. Keskar, K.D. Singh Mudher, J. Alloys Compd. 415 (2006) 244.
[19] N.D. Dahale, M. Keskar, N.K. Kulkarni, K.D.S. Mudher, J. Alloys Compd. 440 (2007) 145.
[20] M. Keskar, N.D. Dahale, K. Krishnan, J. Nucl. Mater. 393 (2009) 328.
[21] R.E. Wilson, S. Skanthakumar, P.C. Burns, L. Soderholm, Angew. Chem.-Int. Ed. 46 (2007) 8043.
[22] M.S. Wickleder, B. Fourest, P.K. Dorhout, in: third ed., in: L.R. Morss, N.M. Edelstein, J. Fuger (Eds.), The Chemistry of the Actinide and Transactinide Elements, vol. 1, Springer, Dordrecht, 2006, pp. 52–160.
[23] M.S. Kazimi, Am. Sci. 91 (2003) 408.
[24] R. Hargraves, R. Moir, Am. Sci. 98 (2010) 304.
[25] H. Müller-Buschbaum, Z. Anorg. Allg. Chem. 635 (2009) 1065.
[26] S. Launay, M. Quarton, Powder Diffr. 13 (1998) 107.
[27] Z. Allan, H.T. David, J. Chem. Phys. 40 (1964) 501.
[28] M. Huyghe, M.R. Lee, M. Quarton, F. Robert, Acta Crystallogr. Sect. C 47 (1991) 244.
[29] M. Huyghe, M.R. Lee, M. Quarton, F. Robert, Acta Crystallogr. Sect. C 47 (1991) 1797.
[30] C.K. Moller, Acta Chem. Scand. 8 (1954) 81.
[31] M. Huyghe, M.R. Lee, S. Jaulmes, M. Quarton, Acta Crystallogr. Sect. C 49 (1993) 950.
[32] B.G. Brandt, A.C. Skapski, Acta Chem. Scand. 21 (1967) 661.
[33] Bruker, APEX2 Version 2009.5-1 and SAINT Version 7.34a Data Collection and Processing Software, Bruker Analytical X-Ray Instruments, Inc., Madison, WI, USA, 2009.
[34] Bruker, SMART Version 5.054 Data Collection and SAINT-Plus Version 6.45a Data Processing Software for the SMART System, Bruker Analytical X-Ray Instruments, Inc., Madison, WI, USA, 2003.
[35] G.M. Sheldrick, Acta Crystallogr. Sect. A 64 (2008) 112.
[36] L.M. Gelato, E. Parthe, J. Appl. Crystallogr. 20 (1987) 139.
[37] J.C. Fitzmaurice, I.P. Parkin, New J. Chem. 18 (1994) 825.
[38] T.L. Cremers, P.G. Eller, R.A. Penneman, Acta Crystallogr. Sect. C 39 (1983) 1165.
[39] K. Mucker, G.S. Smith, Q. Johnson, R.E. Elson, Acta Crystallogr. Sect. B 25 (1969) 2362.
[40] H.J. Whitfield, D. Roman, A.R. Palmer, J. Inorg. Nucl. Chem. 28 (1966) 2817.
[41] Q. Huang, S.J. Hwu, X.H. Mo, Angew. Chem.-Int. Ed. 40 (2001) 1690.
[42] S.J. Hwu, M. Ulutagay-Kartin, J.A. Clayhold, R. Mackay, T.A. Wardojo, C.J. O'Connor, M. Krawiec, J. Am. Chem. Soc. 124 (2002) 12404.
[43] M. Pages, W. Freundlich, J. Inorg. Nucl. Chem. 34 (1972) 2797.
[44] P.K. Dorhout, G.L. Rosenthal, A.B. Ellis, Solid State Ionics 32/33 (1989) 50.
[45] T.Y. Shvareva, P.M. Almond, T.E. Albrecht-Schmitt, J. Solid State Chem. 178 (2005) 499.
[46] N. Ding, M.G. Kanatzidis, Nat. Chem. 2 (2010) 187.
[47] Y. Moro-Oka, W. Ueda, in: D.D. Eley, H. Pines, W.O. Haag (Eds.), Advances in Catalysis, vol. 40, Academic, San Diego, USA, 1994, pp. 233–273.
[48] A.W. Sleight, K. Aykan, D.B. Rogers, J. Solid State Chem. 13 (1975) 231.